Combustors for Micro-Gas Turbine Engines

Ian A. Waitz
Associate Professor,
Massachusetts Institute of Technology,
Gas Turbine Laboratory,
Cambridge, MA 02139

Gautam Gauba
Consultant,
Arthur D. Little Inc.,
Cambridge, MA 02140

Yang-Sheng Tzeng
Graduate Research Assistant,
Massachusetts Institute of Technology,
Gas Turbine Laboratory,
Cambridge, MA 02139

The development of a hydrogen-air microcombustor is described. The combustor is intended for use in a 1 mm^2 inlet area, micro-gas turbine engine. While the size of the device poses several difficulties, it also provides new and unique opportunities. The combustion concept investigated is based upon introducing hydrogen and premixing it with air upstream of the combustor. The wide flammability limits of hydrogen-air mixtures and the use of refractory ceramics enable combustion at lean conditions, obviating the need for both a combustor dilution zone and combustor wall cooling. The entire combustion process is carried out at temperatures below the limitations set by material properties, resulting in a significant reduction of complexity when compared to larger-scale gas turbine combustors. A feasibility study with initial design analyses is presented, followed by experimental results from 0.13 cm^3 silicon carbide and steel microcombustors. The combustors were operated for tens of hours, and produced the requisite heat release for a microengine application over a range of fuel-air ratios, inlet temperatures, and pressures up to four atmospheres. Issues of flame stability, heat transfer, ignition and mixing are addressed. A discussion of requirements for catalytic processes for hydrocarbon fuels is also presented.

1 Introduction

Micromachining of silicon and refractory ceramics is enabling the development of a new class of miniature devices including micromotors, microvalves, pressure transducers, microaccelerometers, and numerous others (Bryzek et al., 1994). Arguably one of the most challenging and innovative endeavors being pursued in this area is the development of microscale turbomachines as described by Epstein et al. (1995). These devices include micromotor compressors, micro-turbine generators, micro-gas turbines, microrefrigerators, and micro-rocket engines. Several of these heat engine applications require conversion of chemical energy to kinetic and thermal energy, and thus it is necessary to develop combustion strategies suitable for use in these miniature devices.

The objective of this paper is to elucidate many of the challenges and opportunities associated with combustion in small volumes, and to offer possible strategies for microcombustion systems. Following a brief overview of micro-gas turbine technology in Section 1.1, the specific challenges and opportunities for microcombustor development are discussed in Section 1.2. Two viable microcombustion alternatives are presented in Section 2: the first based upon hydrogen-air combustion (Section 2.2.1), and the second upon a catalytic hydrocarbon-air reaction (Section 2.2.2). Results from experiments in a full-scale microcombustor are presented in Section 3 to provide a first proof-of-concept demonstration. The paper ends in Section 4 with a summary, conclusions and recommendations for future research.

1.1 Overview of Microengine Technology. The primary motivation for the work described in this paper is the development of micro-gas turbine generators capable of producing 10-100 watts of electrical power while occupying less than 1 cm^3 and consuming approximately 7 grams of jet fuel per hour. If such a device is successfully developed, it will possess an energy density 10 times that available from the best existing batteries. Feasibility studies, preliminary designs, and performance estimates have been discussed in detail by Epstein et al. (1995) and Groshenry (1995). In this section, we present only a short review of the technology in order to establish the design goals and constraints for a microcombustor.

Microengine technology has been enabled by the advent of micromachining processes for refractory, structural ceramics such as silicon nitride (Si_3N_4) and silicon carbide (SiC). These materials have excellent mechanical, thermal, and chemical properties for hostile environment applications, and indeed have been the focus of several development efforts for larger-scale devices (Nakazawa et al., 1996; Measley and Smyth, 1996; Tanaka et al., 1996). Components manufactured from these materials can survive uncooled operation at temperatures as high as 1750 K (Tanaka et al., 1996; The Carborundum Company, 1989). Therefore, use of these materials for a micro-gas turbine engine insures sufficient power per unit air flow to allow for useful power output despite the fact that individual component performances are likely to be below those of larger machines. Further, millimeter-size parts can be fabricated with 1–2 micron tolerances using micromachining processes (Juan et al., 1996), providing a dimension-to-tolerance ratio that is competitive with larger-scale turbomachinery components. Micromachined parts however, are typically limited to extrusions of two-dimensional shapes, thus the geometries are somewhat rudimentary when compared to their larger counterparts.

An example of a micro-gas turbine design is shown in Fig. 1. The overall dimensions of the device are roughly 1 cm in diameter and 3 mm in height. This design is the result of a preliminary analysis for an engine geometry and layout that are compatible with individual component characteristics and constraints of micromachining technology. Thus the design embodies trade-offs between power output requirements, cycle parameters, material limitations, physical dimensions and manufacturing processes. The device consists of a radial flow compressor and a radial flow turbine mounted on the same shaft and separated by a combustor. An integral electrostatic induction generator is located on the top face of the compressor shroud. The combustor is the largest component of the engine.

The characteristics of the micro-gas turbine are summarized in Table 1; the device is a factor of 500 smaller than conventional gas turbine engines. Preliminary analyses by Epstein et al. (1995) suggest that such a machine operating at a tip speed of 500 m/s, with a compressor pressure ratio of 4.5:1 and a

Contributed by the Fluids Engineering Division for publication in the JOURNAL OF FLUIDS ENGINEERING. Manuscript received by the Fluids Engineering Division October 14, 1996; revised manuscript received September 11, 1997. Associate Technical Editor: Wing-Fai Ng.

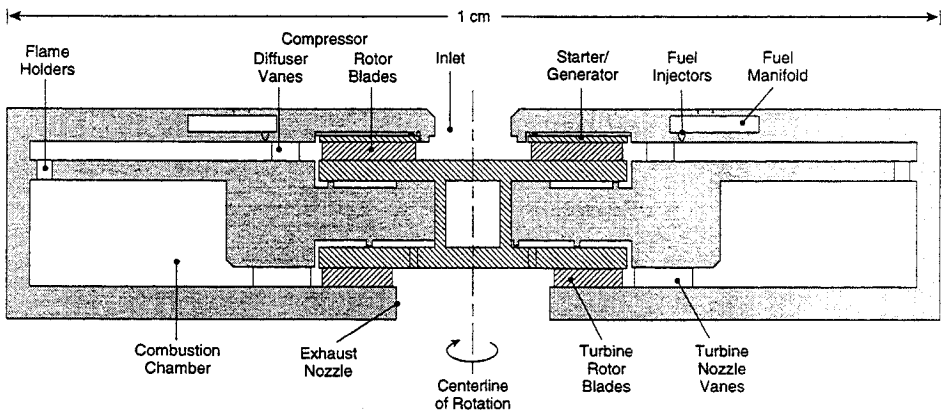

Fig. 1 Schematic of a micro-gas turbine and electrical generator

turbine inlet temperature of 1600 K, may be capable of producing 10-20 watts for a canonical inlet area of 1 mm^2.

The overall goal is to develop a complete microengine system that is contained within a volume on the order of 1 cm^3. Before such a device can be realized however, many difficulties must be overcome. Micro-gas turbines and other applications of this technology are not simply scaled-down larger machines. The small size and constraints on fabrication and testing pose many challenges: the surface area-to-volume ratio is increased, viscous effects are more important, time-scales are shorter, and the range of three-dimensional shapes that can be fabricated is limited. All of these effects either directly or indirectly impact the selection and development of appropriate combustion strategies for a microengine.

1.2 Challenges and Opportunities for Microcombustor Development. The functional requirements of a microcombustor are similar to those of a typical gas turbine combustor. Primarily, chemical energy must be converted into thermal and kinetic energy with high efficiency and low total pressure loss. In addition, there are requirements for introduction and mixing of fuel and oxidizer, reliable and smooth ignition, wide flammability limits so the flame stays lit over a range of operating conditions, low pollutant emissions, and freedom from combustion instabilities. Likewise, the principal constraints on microcombustor design mirror those of the larger-sized counterpart, including the maintenance of low-stressed, cooled structures, minimal weight, and an overall shape and size that are compatible with the rest of the engine layout.

A comparison between design parameters of a conventional gas turbine combustor and those of a microcombustor are shown in Table 2. The parameters listed for the conventional combustor are representative of a modern 30:1 pressure ratio gas turbine engine. The estimates cited for the microcombustor were obtained by making conservative assumptions about achievable performance and size of a microengine operating with a total pressure ratio of 4.5:1. Compared to the larger-scale device, the size of the microcombustor has been reduced by a factor of 100 and the volume by over 6 orders of magnitude. The space heating rate is 10 times larger than that of current technology aircraft gas turbine combustors.

The differences between design parameters listed in Table 2 for the micro and conventional applications are largely due to the reduction in scale, but are also influenced by the relative size of the combustor with respect to the engine, the cycle pressure ratio, and material temperature limitations. These effects are discussed in greater detail in the following sections.

1.2.1 Shorter Residence Time for Mixing and Combustion. The most significant and technically challenging aspect of a microcombustor is its limited residence time. If the dimensions of a conventional engine were to be reduced by a factor of 500, while maintaining the same mass flow rate per unit area, then the flow residence time within the combustor would be approximately 0.05–0.1 ms. This is on the same order as the characteristic chemical kinetic time scale for hydrocarbon-air reactions (0.01–0.1 ms). Thus for the microengine, it will be necessary to increase the relative size of the combustor compared to the engine.

The required increase in relative combustor size can be approximated using a simplified scaling for combustor residence time given by Kerrebrock (1992)

$$\tau_{res} \propto \frac{L \cdot (A_b/A_2) \cdot \pi_c^{1/\gamma}}{\dot{m}/A_2} \tag{1}$$

Nomenclature

A_2 = compressor flow area
A_b = combustor cross-sectional area
A_c, A_h = pre-exponential factors for reaction rates
A_s = surface area [m^2]
C_p = specific heat at constant pressure [J/kg·K]
d_h = hydraulic diameter [m]
Da_c = catalytic Damkohler number
Da_h = homogeneous Damkohler number
E'' = rate of energy/heat flux [W]
$\dot{E}$ = rate of energy/heat generation [W]
h = convective heat transfer coefficient [$W/m^2 \cdot K$]
J_D = mass transport number
J_H = heat transport number
k = thermal conductivity [W/m·K]
L = length [m]
$\dot{m}_a$ = air flow rate [kg/s]
$\dot{m}_f$ = fuel flow rate [kg/s]
Nu_d = Nusselt number based on diameter
$\dot{Q}$ = volumetric rate of energy/heat generation [W/m^3]
Q_f = fuel heating value [J/kg]
Re_d = Reynolds number based on diameter
T = flow temperature [K]
T_w = wall temperature [K]
T_{T3} = compressor exit temperature [K]
T_{T4} = turbine inlet temperature [K]
V_o = reference velocity [m/s]
Vol = volume [m^3]
α = mass transfer coefficient [m/s]
η = combustor efficiency
π_c = compressor pressure ratio
γ = ratio of specific heats
ρ_o = reference density [kg/m^3]
τ_{res} = combustor residence time
ϕ = equivalence ratio

Table 1 Performance estimates for a micro-gas turbine engine

Type	Single spool turbojet/turbogenerator
fuel	H_2
recuperator	No
engine weight	1 g
inlet area	1 mm^2
air flow rate	0.2 g/s
pressure ratio	4.5:1
turbine inlet temperature	1600 K
power output (electrical)	10–20 W
thrust (as turbojet)	0.1~0.2 N
fuel consumption	7 g/hr
specific fuel consumption	0.45 kg/kW·hr
thrust/wt	20:1
energy/air flow	84 J/g

Note that either the length or the area of the microcombustor must be enlarged by a factor of 4 solely to account for the reduced pressure ratio of the cycle (4.5:1 compared to 30:1 for the conventional application), for fixed mass flow per unit area. It will require a further ten-fold increase in either microcombustor length or area to raise the combustor residence time by a factor of 10. This will result in a residence time of 0.5 to 1 ms which is several times larger than the chemical time scale. Therefore, if a full-sized engine is scaled down by a factor of 500, the volume of the microcombustion chamber must grow relative to the engine by a factor of approximately 40 to provide sufficient residence time for complete reaction. Even after this factor of 40 increase, the entire microengine can still be contained in less than 1 cm^3 volume.

Note, however, that the residence time in conventional gas turbine combustors is not driven primarily by the reaction rate. Rather it is governed by requirements for fuel-air mixing as well as dilution with air to reduce the flow temperature and meet efficiency and emissions requirements. Indeed, of the typical 5–8 ms combustor residence time in a conventional gas turbine, approximately 3–5 ms is devoted to fuel vaporization and mixing, and about 2–3 ms to mixing of dilution air (Dodds and Bahr, 1990; Lefebvre, 1983). Thus if conventional combustion strategies are adopted for the microengine application, augmenting the fuel-air mixing rate will be necessary.

1.2.2 Heat Losses Due to the High Surface-to-Volume Ratio. Energy loss due to heat transfer at the walls of the combustion chamber is typically neglected in the design of conventional gas turbine engines. However, for the combustor designs presented in Table 2, the surface area-to-volume ratio, which is proportional to the inverse of the hydraulic diameter, increases from 3–5 m^{-1} for the large-scale combustor to 500 m^{-1} for the microcombustor, and thus heat transfer losses may pose a significant problem.

The effects of surface heat loss on combustion have been investigated in several studies. In premixed gases, flame extinction occurs when the amount of heat liberated by combustion, minus the heat transferred from the gas, no longer exceeds the amount needed to ignite the mixture (Dodds and Bahr, 1990; Ballal and Lefebvre, 1979). Studies of premixed combustion in flame tubes (Zeldovich et al., 1990; Zamaschikov, 1995) have shown that if the inner diameter of a flame tube is less than some critical size, heat transfer from the flame front to the tube wall quenches the reaction. Below this critical diameter, a combustion wave can only be stabilized through external heating of the tube wall.

For a combustor, the ratio of surface heat transfer losses to total heat released in the combustion process can be written as

$$\frac{E''}{\dot{E}} = \frac{A_s h(T - T_w)}{Vol \cdot \dot{Q}} \tag{2}$$

For given fuel, equivalence ratio, inlet temperature, and pressure, the energy per unit volume released in the combustion process, $\dot{Q}$, is constant. Since the dependence of Nusselt number on Reynolds number differs between the flow regimes of a conventional combustor and a microcombustor, the turbulent flow case, which is more sensitive to Reynolds number

$$\mathrm{Nu}_d \propto \sqrt[5]{\mathrm{Re}_d^4} \tag{3}$$

is adopted for both flow conditions. As a result, the convective heat transfer coefficient

$$h = \frac{k \cdot \mathrm{Nu}_d}{d_h} \tag{4}$$

is inversely proportional to the fifth root of the hydraulic diameter. Finally, if the temperature difference between the wall and the flow is assumed to be roughly equal for the two combustors, then the ratio of heat lost to that generated would scale with the hydraulic diameter as follows:

$$\frac{E''}{\dot{E}} \propto \frac{1}{d_h^{1.2}} \tag{5}$$

The hydraulic diameter of the microcombustor is on the order of 2 mm, several hundred times smaller than that of a conventional gas turbine combustor. Thus the ratio of heat lost to heat generated will be about 2 orders of magnitude greater than that of typical combustors. This is likely to influence the performance of a microcombustor in two ways: 1) typical large-scale combustor efficiencies of greater than 99.9 percent may not be feasible due to the significant surface heat transfer losses, and 2) flammability limits are likely to be affected because of flame quenching.

1.2.3 Use of Refractory Structural Ceramics. A noteworthy item listed in Table 2 is the maximum material temperature allowable for each application: 1200 K for uncooled structures in current gas turbines, and approximately 1600 K for the structural refractory ceramics targeted for use in micro-gas turbine engines. The increase in operating temperature projected for the microengine structure alleviates some of the requirements for combustor wall cooling.

Fracture failure has generally hindered the use of refractory ceramics for large-scale applications. Parts with larger volumes statistically entail flaws that are greater in quantity, larger in size, and deeper in location (Scott, 1979). Failure of ceramic

Table 2 Comparison between conventional and microcombustors

Design requirement (sea level takeoff)	Conventional combustor	Microcombustor
length	0.3 m	0.003 m
volume	6×10^{-2} m^3	4×10^{-8} m^3
cross-sectional area	0.2 m^2	4×10^{-5} m^2
inlet total pressure	30 atm	4.5 atm
intlet total temperature	800 K	500 K
mass flow	55 kg/s	20×10^{-4} kg/s
average flow speed	40–60 m/s	6 m/s
residence time	5–8 ms	0.5 ms
efficiency	>99.5%	>99.5%
combustor pressure ratio	>0.95	>0.95
exit temperature	1800 K	1500 K
allowable wall temperature	1200 K	1600 K
space heating rate (kW/m^3/atm)	3.8×10^4	3.3×10^5

parts typically occurs through propagation of existing material imperfections, but this is less of a concern for microengines because of the small component size. Quality control and refinement during manufacturing can be more readily applied to reduce inherent flaws, so the structural capabilities of these high temperature refractory ceramics can be more fully realized.

2 Combustors for Microengines

Before discussing the proposed combustion strategies for microengines, it is instructive to review the physical basis for the combustion scheme that is currently employed in most gas turbine applications.

2.1 Combustion in Large-Scale Engines. The enthalpy rise requirement of a gas turbine combustor is set by the cycle pressure ratio, properties of the working fluid and the fuel, and material limitations. A balance of these influences is described by the equation

$$\frac{\dot{m}_f}{\dot{m}_a} = \frac{C_p}{Q_f}(T_{T4} - T_{T3}) \tag{6}$$

an expression of the first law of thermodynamics. The required fuel-air ratio is a function of the combustor inlet temperature (T_{T3}), which is set by the compressor pressure ratio, the combustor exit temperature (T_{T4}), which is typically set by maximum material temperature limits downstream of the combustor, and properties of the fuel and air (Q_f, and C_p, respectively). For gas turbine applications, the fuel-air ratio mandated by these constraints typically falls between 0.015 and 0.045 over the operating range of the engine. This proportion may also be expressed as an equivalence ratio

$$\phi = \frac{\dot{m}_f/\dot{m}_a}{(\dot{m}_f/\dot{m}_a)_{\text{stoichiometric}}} \tag{7}$$

which would then range between 0.21 and 0.63.

The combustion strategies employed in current combustors are set to a large extent by the fact that most hydrocarbon-air mixtures will not burn at equivalence ratios less than approximately 0.5. The restrictive flammability range mandates a two-zone combustion scheme: a primary zone with relatively high equivalence ratio, which also implies high temperatures beyond material limits, and a secondary or dilution zone where additional air is supplied to reduce the mixture temperature to fall within material limits. The dilution zone is also the region where pollution processes are of critical concern. These factors lead to a residence time requirement of between 5 and 8 ms which is relatively independent of the physical size of the engine.

2.2 Combustion Strategies for Microengines. Turning to a discussion of the microcombustor applications, the strategies presented are based upon three general concepts: 1) increasing the size of the combustor relative to the engine to increase residence time, 2) premixing, and 3) lean burning. Removal of fuel-air mixing from the combustion chamber is driven by the severe residence time requirements for the micro application, and the realization that a large part of the residence time in current combustors is devoted to mixing. However, if the reactants are mixed upstream of the combustor, then the stability benefits of a near stoichiometric primary zone are lost. Two alternatives for offsetting this difficulty and achieving stable burning at low equivalence ratios are the use of hydrogen fuel, and the use of hydrocarbons with the assistance of surface catalysis. Concepts based upon these ideas are discussed in Sections 2.2.1 and 2.2.2, respectively.

2.2.1 Lean Burning Hydrogen-Air System. Hydrogen is an ideal fuel in many respects. Table 3 compares selected fuel properties of hydrogen with a typical hydrocarbon. Hydrogen has a greater heating value, more rapid rate of vaporization,

Table 3 Comparison of selected microengine fuels (winter, 1990)

Fuel property*	Hydrogen/ air mixture	Hydrocarbon/ air mixture
nominal composition	H_2	$CH_{1.8}$
fuel specific heating value (kJ/g)	120	42.8
diffusion velcoity (cm/s)	2	0.2
flammability limits (% by volume)	4–75	0.6–4
vaporization rate w/o burning (cm/min)	2.5–5	0.05–0.5
minimum ignition energy (mJ)	0.02	0.25
autoignition temperature (K)	858	500
characteristic reaction time at 5 atm (s)	$1 \times 10^{6-}$	1×10^{5}
flame propagation velocity (cm/s)	300	20
stoichiometric adiabatic flame temperature (K)	2318	2200
fraction of thermal energy radiated (%)	17–25	30–42

*(in air at STP, unless otherwise specified).

faster diffusion velocity, shorter reaction time, a significantly higher flame speed, wider burning limits, lower ignition energy, and radiates less heat to its surroundings. Most importantly, the broad flammability limits remove requirements for a relatively rich primary burning zone followed by a dilution zone as is often necessary for hydrocarbon fuels. For a hydrogen-air reaction to provide a turbine inlet temperature of 1600 K, the required equivalence ratio of 0.34 (assuming no surface heat loss) falls well above the lean flammability limit of $\phi = 0.1$.

Although the diffusion speed of hydrogen in air is an order of magnitude greater than that of a hydrocarbon fuel, providing adequate fuel-air mixing is still a critical requirement. Requisite mixing can be achieved if the hydrogen gas is introduced well upstream of the combustor, possibly even upstream of the compressor. Similar lean, premixed, prevaporized combustors have been developed for hydrocarbon fuels for larger-scale gas turbines to meet low-emissions requirements. Two significant difficulties have been identified in studies of these combustors: lean blowout, and flashback or autoignition at high inlet temperatures (Grieb and Simon, 1990). For the current application, lean blowout is not a concern because of the wide flammability limits for hydrogen-air mixtures. Further, at the low operating pressure of 4.5 atm projected for a micro-gas turbine engine, the combustor inlet temperature is around 500 K, which is below the autoignition temperature for a hydrogen-air mixture. Therefore, introduction and premixing of hydrogen well upstream of the combustor is feasible in a microengine to enable nearly complete mixing of fuel and air.

Adoption of a lean, premixed hydrogen system also results in a significant reduction in complexity because of the higher operating temperatures allowed for the microengine's materials. Transpiration and film-cooling are used in conventional gas turbine combustors to maintain the combustor liner below material temperature limits. However, as discussed in Section 1.2.3, the ceramic materials intended for use in microturbomachinery have a distinct thermal advantage over the materials currently used in gas turbines, and are expected to withstand local wall temperatures in the vicinity of 1600 K. Thus a lean burning hydrogen-air system not only obviates the need for a dilution zone, but also removes any requirement for combustor wall cooling. A turbine inlet temperature of 1500 K permits the entire combustion process to be carried out without exceeding material limits.

While storage requirements currently prohibit the use of hydrogen in commercial aircraft, several studies (Winter, 1990) support its use as a fuel for future transport aircraft. For micro-gas turbines, the use of hydrogen fuel is not necessarily viewed as an endpoint, but rather as a first step to enable the realization of a workable microscale device. This hydrogen-air system is the subject of the experimental development efforts described in Section 3.

2.2.2 Catalytic Hydrocarbon-Air Combustion. To achieve stable, lean combustion with a hydrocarbon fuel, catalytic processes must be employed. During the last 30 years, catalysts have been investigated both for augmenting primary heat releasing reactions in gas turbines and for post-combustion treatment of pollutant emissions in aircraft, automobiles, and power generation applications. The focus here will be on situations where catalytic reactions are used to promote the primary combustion reactions.

Overview of Catalytic Combustion. The principal advantage of using catalysts for primary combustion reactions is their ability to sustain reactions for hydrocarbon-air mixtures that are well below the lean flammability limit for homogeneous gaseous combustion. Indeed, combustion of JP-4 at equivalence ratios as low as 0.1 has been reported (Rosfjord, 1976). This is attractive for large-scale applications because the extended lean flammability limit allows combustion to proceed at relatively low temperatures providing the potential for a factor of 100 decrease in emissions of nitrogen oxides.

Catalytic combustors typically employ proprietary platinum- and palladium-based catalysts on monolithic, parallel channel, substrates. Silicon carbide is a leading substrate material. The residence times in the catalyst bed are typically 5 to 30 ms for tubes with hydraulic diameters on the order of 1 to 4 mm. For combustor inlet temperatures ranging from 650 K to 900 K, combustion efficiencies of greater than 99.5 percent have been reported over a range of fuel-air equivalence ratios that result in adiabatic flame temperatures between 1100 K and 1800 K (e.g., Wampler et al., 1976; Mori et al., 1987).

The important technology limiters for catalytic gas turbine combustors are two-fold. First, the minimum operating temperature of approximately 600 K rules out use of catalysts for combustor inlet conditions corresponding to idle and low power cruise operation. Second, the maximum temperature limit of around 1800 K, set by catalyst and substrate thermal degradation, does not allow use for hydrocarbon mixtures with equivalence ratios greater than around 0.6. In practical devices these limits are offset by using preburners, pilot flames, fuel and air staging, and a variety of other hybrid catalytic/homogeneous combustion concepts.

The reacting flow processes within the catalytic bed are complicated, and a brief review of these is necessary to understand how the processes scale with combustor size. The following discussion is based on descriptions given by Groppo et al. (1993), Rosfjord (1976), and Pfefferle (1978). Consider preheated, premixed air and fuel as it passes through a long channel with catalytic surfaces. Reactants are absorbed by the catalyst, surface reactions occur, and then the products are desorbed and along with heat are transported into the flow by diffusion. Three different regions exist in the channel. Region I: Near the inlet of the channel, the fuel conversion is controlled by the kinetics of the heterogeneous reaction at the surface of the catalyst. The bulk gas temperatures are typically too low to support homogeneous combustion. This region of the flow usually extends for a distance of less than five tube diameters. Region II: As the near-wall gas and substrate temperatures rise, the heterogeneous reaction rates increase. The reaction rates increase to an extent that the fuel conversion is no longer controlled by the surface reaction rate, but rather by the rate at which new gas phase reactants are transported to the surface. Pfefferle (1978) notes that, for any reasonably active catalyst at temperatures above 800 K, the catalytic reaction at the wall will be limited solely by the rate of mass transfer. This diffusion limited region extends for 10–100 tube diameters in typical catalytic combustors. Region III: Further downstream, as heat continues to diffuse into the bulk gas flow, thermal ignition of homogeneous or gas phase reactions occurs. These homogeneous reactions are initiated at bulk gas temperatures in the range of 1200–1300 K (Pfefferle, 1978) which is far below the value of 1600 K, the minimum adiabatic flame temperature typically associated with mixtures at the lean flammability limit.

Cerkanowicz, Cole, and Stevens (1977) present several dimensionless groups that are useful for scaling the performance of catalytic combustors. The reaction in Region I is primarily dependent on the catalytic Damkohler number, Da_c, the ratio of residence time to the characteristic heterogeneous reaction time:

$$Da_c = \left(\frac{L}{V_o}\right)\left(\frac{A_c e^{-E_c/RT_o}}{d_h}\right) \tag{8}$$

Because of the dependence of the reaction rate on surface area, $Da_c \propto 1/d_h$ for fixed residence time. The transition from Region I to Region II, and the progression of the reaction in Region II are expected to scale with the mass transport number which is the ratio of the characteristic residence time of the gas in the reactor to the mass transport time

$$J_D = \left(\frac{L}{V_o}\right)\left(\frac{\alpha}{d_h}\right) \tag{9}$$

and the heat transfer number

$$J_H = \left(\frac{L}{V_o}\right)\left(\frac{k}{\rho_o C_p}\frac{1}{d_h}\right) \tag{10}$$

which is the ratio of the residence time of the gas to the characteristic heat transfer time. Both the heat and mass transfer scale inversely with the hydraulic diameter, and thus both are favored as the size of the tube is decreased, as is the overall progression to the homogeneous reaction region. Finally in Region III the process scales with the homogeneous Damkohler number, Da_h the ratio of gas residence time to the homogeneous reaction time.

$$Da_h = \left(\frac{L}{V_o}\right)\left(\frac{A_h[\text{fuel}]^a[O_2]^b e^{-E_h/RT_o}}{[\text{fuel}]_o}\right) \tag{11}$$

For fixed residence time, Da_h is independent of the scale of the device.

Application to Microengines. Based on the preceding discussion of performance and scaling of catalytic combustion systems, the following conclusions can be drawn with respect to a microengine application. The size of the combustor relative to the engine can be increased to obtain a factor of 10 increase in residence time, as was proposed for the hydrogen system. However, the resultant residence time, at 0.5 ms, will still be an order of magnitude less than that in any successfully demonstrated catalytic combustion systems. Second, the combustor inlet temperature of 460 to 500 K in the microengine application is below the 600 K limit required for catalytic ignition. We will discuss each of these challenges in turn, beginning with the low residence time.

The reduced residence time is largely offset by the favorable effects associated with the high surface area-to-volume ratio of the microcombustor, including order of magnitude increases in both the heterogeneous Damkohler number and the nondimensional heat and mass transfer rates that are the primary controlling parameters for the rate of reaction in the system. This suggests that catalytic combustion of hydrocarbons can be completed for flow residence times on the order of 1 ms if the hydraulic diameter of the flow path is reduced by an order of magnitude from larger-scale applications. For the microengine application then, the catalytic flow passages should be approximately 100 microns in diameter. Manginell et al. (1996) have used chemical vapor deposition technology to apply platinum

catalysts to micromachined polysilicon, providing proof that miniature catalytic elements can be microfabricated.

The second problem mentioned above was that the combustor inlet temperature was too low to support catalytic ignition. However, the experimental results presented in Section 3.4 suggest that, for the current configuration, enough heat transfer may be occurring between the combustor and the compressor exit flow passage to overcome this difficulty. If not, a recuperator can be employed. A recuperator is a heat exchanger used to transfer waste heat in the turbine exhaust to the compressor exit flow prior to its entrance into the combustor. Recuperated cycles can provide significantly higher thermal efficiency for low pressure ratio engines because of the relatively large difference in temperature between the combustor exit flow and the turbine exhaust. For the microengine with a 4.5:1 pressure ratio, the compressor exit flow will be approximately 460 K and the turbine exhaust approximately 1200 K, so heat exchangers with efficiencies as low as 20% will allow catalytic combustor operation. A typical heat exchanger efficiency reported in the literature for 50 kW automotive gas turbine applications is about 90% (AlliedSignal Aerospace Company, 1988; Allison Gas Turbine Division, 1988), suggesting that sufficient heat exchanger efficiency can be attained to enable catalytic combustion of hydrocarbons.

The envisioned configuration for a recuperated, catalytic hydrocarbon combustion system is shown in Fig. 2. The compressor exit flow exchanges heat with the engine exhaust before passing into a catalytic combustor. The catalytic combustor is in the form of a radial labyrinth. An additional benefit of such a system is that a large fraction of the heat lost from the walls of the combustion chamber can be retained in the cycle thus improving the overall efficiency of the chemical to thermal energy conversion process. The primary drawback of this system is its geometrical complexity, which may pose a significant challenge to existing microfabrication technology.

3 Hydrogen-Air Microcombustor Experiments and Simulations

A microcombustor test rig was developed to study combustion phenomena for microengine applications. The apparatus and diagnostics are described in Sections 3.1 and 3.2, respectively. Numerical simulations of the flowfield are presented in Section 3.3, followed by initial experimental results for lean, premixed hydrogen-air combustion in Section 3.4.

3.1 Apparatus. A schematic of the model microcombustor is presented in Figure 3. As depicted in the figure, the model consists of a series of plates stacked on top of each other. The hydrogen-air mixture is introduced into the dump combustor through a ring of holes in the combustor inlet plate. After combustion, the flow exits axially. This differs from the flow in the microengine shown in Fig. 1 where the combustion products exit radially into the turbine. Two model microcombustors were constructed, one of silicon carbide, which is the proposed material for the micro-gas turbine, and the other of steel, which allowed easier addition of diagnostics since it was less troublesome to machine. The volume of both combustors was approximately 0.13 cm^3. Likewise, two combustor inlet plates were

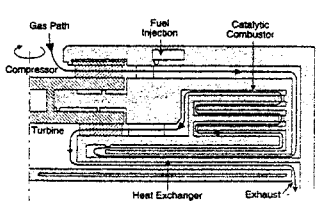

Fig. 2 Schematic of a recuperated microengine with a catalytic combustor for burning hydrocarbon fuels

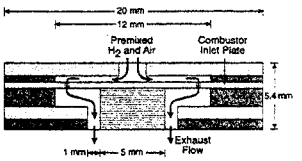

Fig. 3 Schematic of the model microcombustor

manufactured, a 0.4 mm thick steel piece with 24 combustor inlet holes of 0.4 mm diameter around a circle of 5 mm radius, and a 0.5 mm thick silicon carbide plate with 40 inlet holes of 0.38 mm diameter also around a circle of 5 mm radius. The large backward facing area of the inlet plates was designed to set up recirculation zones to provide flameholding.

The apparatus for holding the microcombustor is shown in Fig. 4. The microcombustor plates are held together in compression by a spring. This modular design permits replacement of plates to simplify the task of conducting parametric studies for various geometric configurations. The residence time for the microcombustor flow can be adjusted by adding or removing plates, thereby changing the flowpath length and combustor volume. The downstream side of the combustor is supported by a clear quartz tube to allow limited visual access to the combustor exit flow field. The entire combustor rig is housed in a water-cooled pressure chamber to enable testing at elevated pressures. Visual access is provided by a quartz window.

3.2 Diagnostics and Ignition. Due to the small size and restrictive geometry of the microcombustor, diagnostics for the combusting flow were difficult to apply. Two diagnostic techniques were used: 0.25 mm type K thermocouples and an ionization probe. Temperature measurements included inlet and exit flow temperature, combustion chamber temperature, and combustor wall temperature. The ionization probe was used for evaluating whether a flame existed within the microcombustor. A schematic of the steel combustor illustrating the location of some of the thermocouples, the ion probe, as well as an ignitor, is presented in Fig. 5. For the silicon carbide microcombustor, only a single thermocouple and an ignitor were used. Both the thermocouple and the ignitor were introduced axially into the exit of the combustion chamber. Additional details of these measurement techniques and the ignition procedure are discussed below.

Generally, the temperature indicated by a thermocouple probe is not the same as the gas temperature because of the energy exchange between the thermocouple probe and the surrounding environments. In steady-state, the temperature attained by the probe is a net result of convective energy transfer from the surrounding gas, radiative energy flux to the cooler walls, and

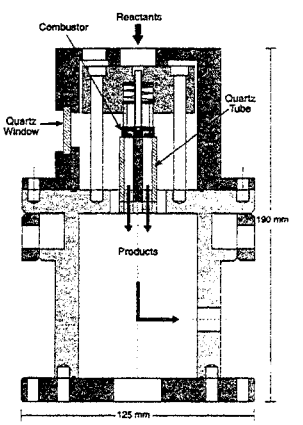

Fig. 4 Schematic of the microcombustor testing facility

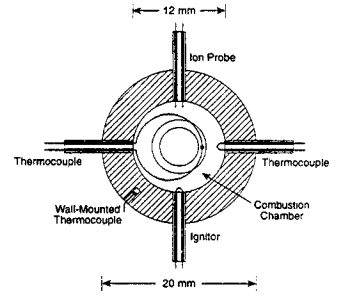

Fig. 5 Microcombustor diagnostics and ignitor layout

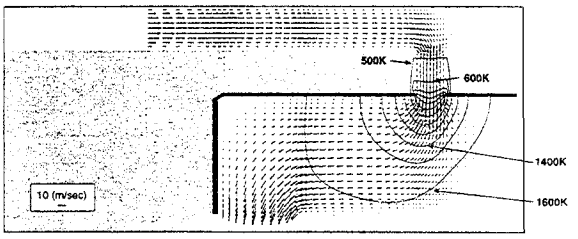

Fig. 6 Results of a numerical simulation showing temperature and velocity fields for the microcombustor for $\phi = 0.4$, $T_{in} = 450$ K, $P_{in} = 1$ atm, and $\dot{m} = 0.045$ g/s

conduction along the wires away from the thermocouple junction. Corrections for these effects must be made to obtain accurate temperature measurements (see, for example, Bradley and Matthews, 1968). For most applications, the length of thermocouple wire exposed to the flow is long enough, and the gradients along the wire are small enough, so that conduction losses are small. However, for the microcombustor, the length of thermocouple wire that protrudes into the flow is limited to only a few millimeters by the scale of the device. Further, the large temperature gradients within the combustion chamber imply unusually high uncertainties in flow temperature measurements due to conduction losses. These uncertainties were aggravated by lack of knowledge of the interior temperature field and additional inaccuracies introduced by the combustor wall measurements. Finally, since radiation corrections require the use of surrounding surface temperatures, they are also impacted by inaccuracies in the combustor wall temperature measurements. Because of these accumulated errors, the estimated uncertainty of the temperature measurements is about ±100 K.

An ionization probe was used to provide a secondary indication of the presence of a flame within the combustion chamber. The underlying concepts of ion probes are discussed in several references (Smy, 1976; Calcote, 1963; Travers and Williams, 1965; Zsak, 1993). The probe consisted of two platinum electrodes separated by an air gap. The two electrodes were maintained at a fixed electrical potential difference. When ionized radicals associated with the combustion zone were present, a current was induced across the air gap, and this was manifest as a change in voltage across a resistance placed in series with the probe.

Ignition of the microcombustor was achieved by resistance heating of a 0.2 mm platinum wire. The ignitor consumed approximately 50 watts of power. Ignition usually occurred in a matter of seconds, but was sensitive to wire location. Ignition occurred more readily if the ignitor was positioned toward the center of the combustion chamber; however, the wires would only survive one test in this position. Moving the ignitor closer to the combustor wall substantially increased its lifetime. As with other experiments reported in the literature (Lewis and von Elbe, 1987) catalysis on the heated platinum may have played a role in the ignition behavior. This will be investigated in future tests.

3.3 CFD Simulations of the Microcombustor. Before presenting experimental results, we illustrate the general features of the flowfield in the microcombustor using results from two-dimensional reacting flow simulations. These simulations were carried out using ALLSPD (Chen et al., 1995), a Navier-Stokes solver incorporating finite-rate chemical kinetics. The code has been validated by personnel at NASA Lewis Research Center (ALLSPD, 1995) for laminar reacting flows like those expected in the microcombustor. A hydrogen-air chemistry model with 9 species and 18 reaction mechanisms was used in the current study. The simulations were conducted for a $\phi = 0.4$ hydrogen-air mixture flowing at a rate of 0.045 g/s. The mixture was specified an inlet temperature of 450 K at atmospheric pressure, to provide a comparison with the microcombustor experiments.

The velocity and temperature fields are shown in Figure 6. Flameholding is seen to occur in the immediate vicinity downstream of the combustor inlet plate hole. The maximum flowfield temperature is 1650 K. The location of the maximum temperatures indicates that there is sufficient time for reactions to be completed well within the current combustor volume of 0.13 cm^3. This conclusion is supported by the results obtained in the experiments, which are discussed in the following section.

3.4 Preliminary Experimental Results. Tests of both the steel and silicon carbide combustors were completed for the two combustor inlet plates described in Section 3.1. Equivalence ratios between 0.4 and 1.0 were tested with mass flow rates from 0.045 g/s to 0.2 g/s for combustor pressures of 1 to 4.5 atmospheres respectively, such that the combustor residence time was maintained at approximately 0.5 ms. These conditions were chosen to correspond to typical microengine operating parameters. All of the tests were carried out by varying the equivalence ratio from $\phi = 1.0$ down to $\phi = 0.4$ in increments of 0.1, and then back up to $\phi = 1.0$ in increments of 0.1. Stable combustion was observed for both the silicon carbide combustor and the steel combustor over the full range of equivalence ratios tested.

Internal temperature measurements obtained with the steel microcombustor are shown in Fig. 7 over a range of hydrogen-air equivalence ratios at atmospheric pressure. The flow rate for the case shown was 0.045 g/s. The measurements have been corrected for radiation and conduction errors, however the uncertainty in these measurements is expected to be ±100 K due to inadequate knowledge of thermal gradients within the combustion chamber as described in Section 3.2. The magnitude of each of the corrections is shown on the plot along with the raw temperature measurement. Also included in the figure are the estimated adiabatic flame temperatures over the range of equiva-

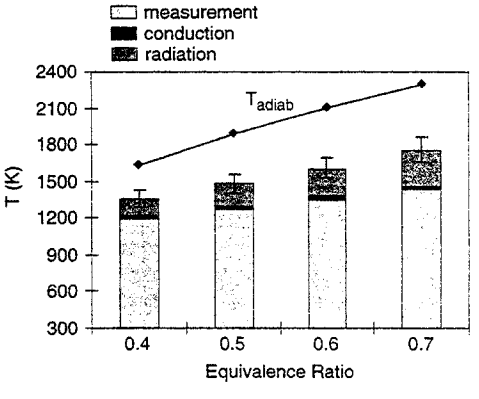

Fig. 7 Exit gas temperatures measured in the hydrogen-air microcombustor

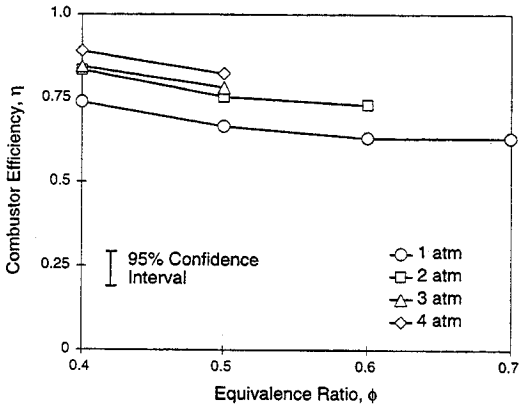

Fig. 8 Combustor efficiency for the microcombustor over a range of pressures and equivalence ratios

lence ratios based on the measured inlet air temperatures. Lack of any visible indication of a flame at the combustor exit (even when the hydrogen was seeded with five percent methane to increase the chemiluminescence) suggests that the combustion efficiency was near one. However, the combustor efficiency was reduced due to heat transfer losses as is suggested by the difference between the corrected temperatures and the adiabatic flame temperatures. This difference increased with increasing equivalence ratio as is expected.

The overall combustor efficiencies associated with these temperature differences fall between 0.7 and 0.9 and are shown plotted in Fig. 8 for the range of equivalence ratios and pressures tested. Results are not presented for many of the higher pressure and equivalence ratio conditions because the associated high temperatures generally resulted in failure of the fine wire thermocouple probes. The combustor efficiency variation with pressure is consistent with the variation in heat transfer coefficients with pressure and flow rate. In sum, despite the low combustor efficiency, both the steel and silicon carbide microcombustors were operated for tens of hours and throughout produced the requisite heat release necessary to support the various heat engine applications that are currently envisioned.

Other observations from these preliminary tests include:

1) The ionization probe indicated the presence of a flame within the combustor over the full range of flow rates tested for equivalence ratios between 0.4 and 1.0. The observed voltage was found to increase with increasing equivalence ratio.
2) At constant flow rate, the choice of the combustor inlet plate did not significantly affect the temperatures measured, probably indicating similar flameholding characteristics, and thus similar temperature fields for the two geometries.
3) The microcombustor plates became sufficiently hot to glow red at equivalence ratios greater than 0.5, and the heat transfer to the inlet gases was significant (on the order of 50 K to 100 K temperature rise). Typically, combustor wall temperatures were about 750 K.
4) The thermocouples located at two different radii within the combustor sensed temperatures that differed by as much as 180 K due to large radial temperature gradients in the combustor. Lack of further knowledge of these gradients is the source for the large errors in conduction corrections quoted for the thermocouples.
5) During some low equivalence ratio conditions, hysteresis in the thermocouple measurements of 200 K was observed suggesting that flameholding did not always occur at the same location within the microcombustor.

4 Summary and Conclusions

Microengines and other miniature thermal devices pose unique challenges and opportunities for combustion in small volumes. The principal difficulties are associated with the limited residence times, and heat transfer losses due to the high surface area-to-volume ratio. Two viable combustion alternatives for microengines were presented in the paper, one that takes advantage of the wide flammability limits of hydrogen-air mixtures, and a second that involves surface catalysis of a hydrocarbon fuel. Both options require an order of magnitude increase in the size of the combustor relative to the engine, and premixing the fuel and the oxidizer to decrease residence time requirements within the combustor. Both combustion strategies also represent significant reductions in complexity from typical gas turbine systems by the removal of requirements for a primary combustion zone where temperatures exceed the material limits.

Preliminary test results from 0.13 cm^3 silicon carbide and steel microcombustors were presented for inlet pressures between 1 and 4 atm. Stable and complete combustion of hydrogen and air was achieved over the full range of equivalence ratios required for a microengine application. Combustor efficiencies between 0.7 and 0.9 were obtained. The low combustor efficiencies were largely a result of heat transfer losses from the walls of the combustor. The experiments provide a first proof-of-concept demonstration for the hydrogen-air system, and suggest that combustion in small volumes for microengine applications is feasible.

The work presented in this paper also highlights the need for significant additional research to more carefully understand flow behavior within the microcombustor. This research would be aided by the development of miniature diagnostic techniques for these flows. Experimental and computational work is continuing with the focus on issues of hydrogen injection and mixing, ignition, catalytic combustion of hydrocarbon fuels, and determination of oxidation rates for silicon carbide in the post-combustion gas environment. A parallel experimental effort is also ongoing using a miniature flame tube apparatus. The flame tube will be used to provide measurements to help validate reacting flow simulations and finite element heat transfer models.

Acknowledgments

We first recognize and thank Professor Alan H. Epstein, both for conceiving and pursuing the concept of microengines, and for being a constant source of encouragement and ingenuity. In addition, we thank the members of the MIT microengines team: Kuo-Shen Chen, Eric Esteve, Luc Frechette, Chuang-Chia Lin, Amitav Mehra, Steve Nagle, Ed Piekos, G. Ananthasuresh, Arturo Ayon, Fredric Ehrich, Stuart Jacobson, Choon Tan, Kenneth Breuer, Mark Drela, Jeffrey Lang, Martin Schmidt, Stephen Senturia, and Mark Spearing, for all they have taught us. The skill and assistance of Viktor Dubrowski, Mariano Hellwig, and James Letendre made the apparatus used in this study possible. We are grateful to Diana Park for superb editing and graphics, and to Holly Anderson for shouldering many of the administrative burdens.

This work was largely supported by the Army Research Office through Grant DAAH04-95-1-0093. We greatly appreciate the interest and encouragement of the technical monitor, Dr. Richard Paur. We also thank the MIT Lincoln Laboratory for providing support for the initial feasibility studies.

References

AlliedSignal Aerospace Company, 1998, "Advanced Gas Turbine AGT Technology Development Project," Final Report to NASA Lewis Research Center, DOE/NASA 0167-12, Mar.

Allison Gas Turbine Division, 1985, "Advanced Gas Turbine AGT Technology Project," Final Report to NASA Lewis Research Center, DOE/NASA 0168-11, Aug.

ALLSPD Demonstration Workshop, Personal Communication, 1995.

Ballal, D. R., and Lefebvre, A. H., 1979, "Weak Extinction Limits of Turbulent Flowing Mixtures," *Journal of Engineering for Power,* Vol. 101, No. 3.

Bradley, D., and Matthews, K. J., 1968, "Measurement of High Gas Temperatures with Fine Wire Thermocouples," *Journal of Mechanical Engineering Science,* Vol. 10, No. 4.

Bryzek, J., Peterson, K., and McCulley, W., 1994, "Micromachines on the March," *IEEE Spectrum,* Vol. 31, No. 5, May.

Calcote, H. F., 1963, "Ion and Electron Profiles in Flames," *Ninth Symposium (International) on Combustion,* The Combustion Institute.

Cerkanowicz, A. E., Cole, R. B., and Stevens, J. G., 1977, "Catalytic Combustion Modeling; Comparisons with Experimental Data," ASME Paper 77-GT-85, Mar.

Chen, K-H., Duncan, B., Fricker, D., Lee, J., and Quealy, A., 1995, ALLSPD-3D, Version 1.0, Internal Fluid Mechanics Division, NASA Lewis Research Center, Nov.

Dodds, W. J., and Bahr, D. W., 1990, "Combustion System Design," *Design of Modern Gas Turbine Combustors,* Mellor, A. M. (Editor), Academic Press Limited.

Epstein, A. H., Groshenry, C., Haldeman, C. W., Schmidt, M. A., Senturia, S. D., Tan, C. S., Waitz, I. A., and Wong, J., 1995, "Microjet Engines," Final Technical Report to MIT Lincoln Laboratory, Massachusetts Institute of Technology.

Grieb, H., and Simon, B., 1990, "Pollutant Emissions of Existing and Future Engines for Commercial Aircrafts," Air Traffic and the Environment—Background, Tendencies and Potential Global Effects, *Proc. of the DLR International Colloquium,* Bonn, Germany, U. Schumann (Ed.), Springer-Verlag.

Groppo, G., Tronconi, E., and Forzatti, P., 1993, "Modelling of Catalytic Combustors for Gas Turbine Applications," *Catalysis Today,* Vol. 17, Elsevier Science Publishers B. V., Amsterdam, pp. 237–250.

Groshenry, C., 1995, "Preliminary Study of a Micro-Gas Turbine Engine," S.M. thesis, Massachusetts Institute of Technology, May.

Juan, W-H., Pang, S. W., 1996, "Released Si Microstructures Fabricated by Deep Etching and Shallow Diffusion," *Journal of Microelectromechanical Systems,* Vol. 5, No. 1, Mar.

Kerrebrock, J. L., 1992, *Aircraft Engines and Gas Turbines,* 2nd ed., MIT Press.

Lefebvre, A. H., 1983, *Gas Turbine Combustion,* Hemisphere Publishing Corporation.

Manginell, R. P., Smith, J. H., Ricco, A. J., Moreno, D. J., Hughes, R. C., Huber, R. J., and Senturia, S. D., 1996, "Selective, Pulsed CVD of Platinum on Microfilament Gas Sensors," Solid State Sensor and Actuator Workshop, Hilton Head, South Carolina, June.

Measley, M. L., and Smyth, J. R., 1996, "Ceramic Gas Turbine Technology Development," ASME paper 96-GT-367.

Mori, K., Kitajima, J., Kajita, S., and Ichihara, S., 1987, "Development of a Catalytic Combustor for Small Gas Turbines," ASME Paper 87-GT-62, May-June.

Nakazawa, N., Ogita, H., Takahashi, M., Yoshizawa, T., and Mori, Y., 1996, "Radial Turbine Development for the 100 kW Automotive Ceramic Gas Turbine," ASME paper 96-GT-366.

Pfefferle, W. C., 1978. "The Catalytic Combustor: An Approach to Cleaner Combustion," *AIAA J. Energy,* Vol. 2, May-June.

Rosfjord, T. J., 1976, "Catalytic Combustors for Gas Turbine Engines," AIAA Paper 76-46, Jan.

Scott, W. D., 1979, "Statistics of the Strength of Brittle Materials," *Design with Brittle Materials,* Mueller, J. I., Kobayashi, A. S., Scott, W. D. (Editors), University of Washington.

Smy, P. R., 1976, "The Use of Langmuir Probes in the Study of High Pressure Plasmas," *Advances in Physics,* Vol. 25, No. 5.

Tanaka, K., Tsuruzono, S., Kubo, T., and Yoshida, M., 1996, "Development and Fabrication of Ceramic Gas Turbine Components," ASME paper 96-GT-446.

The Carborundum Company, 1989, "Physical Properties of Hexoloy® SA Silicon Carbide—Technical Data," The Carborundum Company, November 10.

Travers, B., and Williams, H., 1965, "The Use of Electrical Probes in Flame Plasmas," Tenth Symposium (International) on Combustion, The Combustion Institute.

Wampler, F. B., Clark, D. W., and Gaines, F. A., 1976, "Catalytic Combustion of C_3H_8 on Pt Coated Monolith," *Combustion Science and Technology,* Vol. 14, pp. 25–31.

Winter, C.-J., 1990, "Hydrogen Technologies for Future Aircraft," Air Traffic and the Environment—Background, Tendencies, and Potential Global Atmospheric Effects, *Proc. of the DLR International Colloquium,* Bonn, Germany, U. Schumann (Editor), Springer-Verlag.

Zamaschikov, V. V., 1995, "Combustion of Gases in Thin-Walled Small-Diameter Tubes," *Combustion, Explosion, and Shock Waves,* Vol. 31, No. 1, Jan.-Feb.

Zeldovich, Y. B., Barenblatt, G. I., Librovich, V. B., et al., 1990, *Mathematical Theory of Combustion and Explosion.*

Zsak, T. W., 1993, "An Investigation of the Reacting Vortex Structures Associated with Pulse Combustion," Ph.D. thesis, California Institute of Technology.